Background issues in the design of Muon Collider IRs and Detectors

A brief review of past work

C. Johnstone and N. Mokhov, Fermilab

NFMCC meeting

January 25, 2009

Introduction

One of the most serious technical issues in the design of a muon collider arises from muon decay. In the 2x2 TeV muon collider, with 2×10^{12} circulating muons, 2×10^5 $\mu \rightarrow e\nu\text{-}\nu\text{+}$ decays occur per meter. Immersed in strong magnetic fields, electromagnetic showers deposit ~2 kW/meter in the storage ring, several orders of magnitude more than in upstream systems. Below is a summary of the heat deposited in the different systems of a high-energy muon collider.

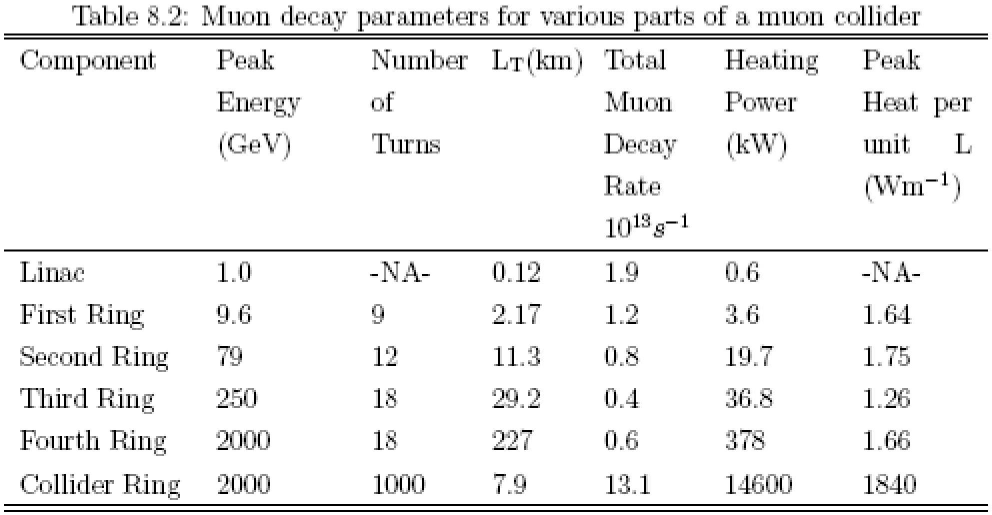

Table 8.2: Muon decay parameters for various parts of a muon collider

Component	Peak Energy (GeV)	Number of Turns	L_T(km)	Total Muon Decay Rate $10^{13} s^{-1}$	Heating Power (kW)	Peak Heat per unit L (Wm^{-1})
Linac	1.0	-NA-	0.12	1.9	0.6	-NA-
First Ring	9.6	9	2.17	1.2	3.6	1.64
Second Ring	79	12	11.3	0.8	19.7	1.75
Third Ring	250	18	29.2	0.4	36.8	1.26
Fourth Ring	2000	18	227	0.6	378	1.66
Collider Ring	2000	1000	7.9	13.1	14600	1840

Heat Generation in Muon machines

- Heat Sources:
  - Muon synchrotron radiation
  - Muon decay: electrons, positrons and associated synchrotron radiation, and neutrinos
  - Muons from the primary beam that hit the vacuum chamber
- The breakdown of heat deposition shows that the SC magnet design is almost completely influenced by muon decay and their synchrotron radiation

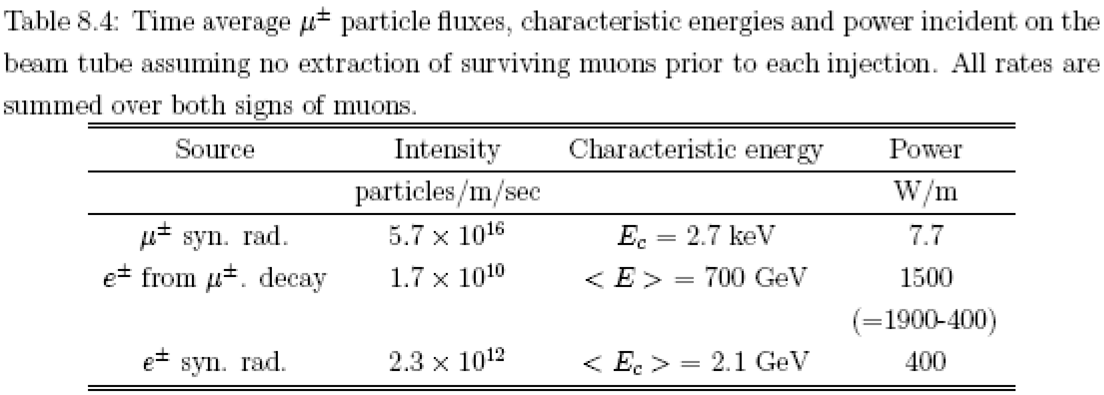

Table 8.4: Time average $\mu^\pm$ particle fluxes, characteristic energies and power incident on the beam tube assuming no extraction of surviving muons prior to each injection. All rates are summed over both signs of muons.

Source	Intensity	Characteristic energy	Power
	particles/m/sec		W/m
$\mu^\pm$ syn. rad.	5.7×10^{16}	$E_c = 2.7$ keV	7.7
$e^\pm$ from $\mu^\pm$. decay	1.7×10^{10}	$< E > = 700$ GeV	1500 (=1900-400)
$e^\pm$ syn. rad.	2.3×10^{12}	$< E_c > = 2.1$ GeV	400

Heat Generation in Muon machines

- LESS THAN 0.1% of the energy from muon decay products can be deposited on the SC coils or its surrounding support structure. Solutions for the heating problem include:
  - Thick tungsten radiation shield to reduce the deposited energy by three orders of magnitude
  - Separate the coils across the midplane
  - Active (background sweep dipoles) and passive (tungsten collimators) insterted between the final focus quadrupoles to shadow/shield the SC.

Tungsten liner

- By itself the thickness of a tungsten liner would be 65 mm to reduce the heat load from muon decay by three orders of magnitude. This implies
  - The warm bore required for 5σ beam is 20 mm.
  - The tungsten liner increases the bore to 160 mm with severe impact on the final focus magnets, optics, and ring impedence.

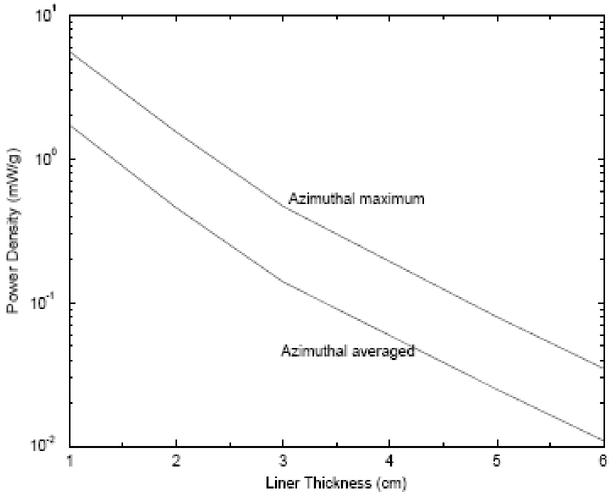

Figure 8.15: Maximum and azimuthal averaged power density in the first SC cable shell in the collider arc *vs* tungsten liner thickness for 2 TeV muon beam decays.

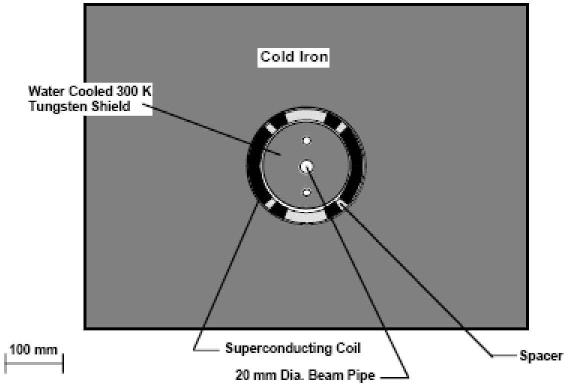

Figure 8.11: A cold iron 8.5 T cosine theta dipole with a 65 mm thick tungsten liner at 300 K

Consequences of enlarged apertures in final focus

- Adding the 6 cm liner increases the difficulty of an already problematic design
  - The nonlinear dynamics dominated by the IR are strongly correlated to the strength of and beam size at the final focus quadrupoles*
  - The beam size at the quadrupole nearest the IP is 2 cm (2.5 σ) and adding 6 cm to the aperture represents a factor of 4 decrease in quadrupole strength, a factor of 4 increase in length, with an approximate corresponding increase in the β function, (square root of the beam size)
  - First-order chromaticity has a linear dependence the peak β function and therefore increases almost linearly with the strength reduction
  - Nonlinear behavior associated with chromatic correction sextupoles can show orders of magnitude increase with severe impact on dynamic aperture

*"Zeroth-Order Design Report for the Next Linear Collider", SLAC-474, Proceeding os the Snowmass Workshop, June-July, 1996.

Open midplane magnet design

- Another approach is to clear the midplane of SC coils
  - The coils are separated in the dipoles such that <0.1% of the energy from muon decay is deposited in the coils or its 4K surrounding support structure
    - The iron return yoke would likely be cold with the heavy supports needed to counteract the attractive forces between coils. The remaining muon decay energy would be deposited in a separate, cooled radiation shield.
  - A corresponding separated coil quadrupole can be designed with 100-200 T/m gradients.
  - The separated coil design clearly impacts detector design due to the larger-radius shielding required on the midplane

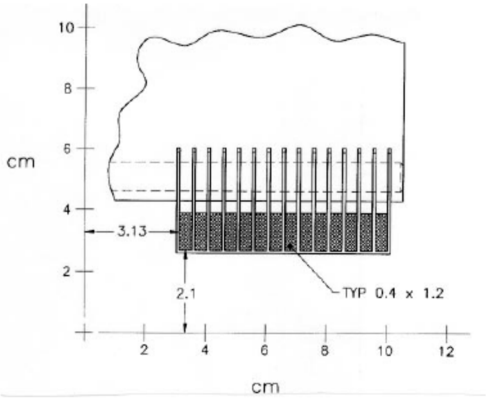

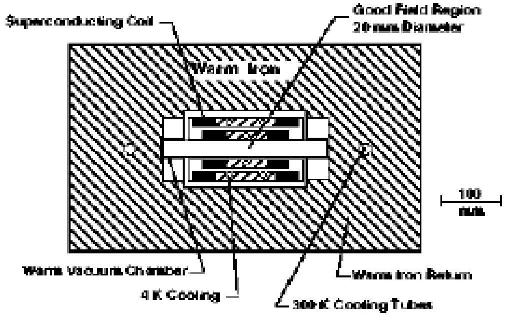

Figure 3: 8.5 T dipole with warm iron and SC coils moved off the mid-plane.

Open midplane design drawbacks

- There are difficulties associated with achieving the desired optics using nonconventional magnets
    - The muon collider is extremely sensitive to end or fringe field effects from such large magnet apertures
    - Fringe field effects change the dynamics completely of the collider ring
    - Open mid-plane magnets cannot necessarily be modeled using conventional component exhibit high-order multipole content.
    - An accurate simulation would likely require the actual field map from TOSCA. Once a field map is required, optimization of parameters entirely within existing optical codes is not currently implemented nor is there a straightforward approach to implement..

Combined Approach

- By far the most effective approach is a combined passive and shielding design consisting of:
  - Tapered liners in final focus quads
  - Background sweep dipoles
    - Positioned on either side of the final focus quadrupoles, a pair of 15-m long, 8.5T background dipoles had to be placed 1 m upstream of the final focus to remove background from the arcs and the long preceding drift. (This is a bucked pair of dipoles to keep the dispersion function under control in the long drift.)
  - Tungsten collimators sandwiched between quadrupoles
    - 15-cm long with a 4σ aperture to shadow completely the SC final focus quads with a 5σ aperture.
  - Tungsten collimators within the detector with the aspect of the two nozzles on either side of the IP

Results: Combined Approach

- The combined effect allowed the tungsten liner to be reduced to 2 cm
  - Promoting a factor of 2 decrease in linear chromaticity and sextupole strength
  - Higher order chromaticities which require higher-multipole correction dropped by two orders of magnitude.

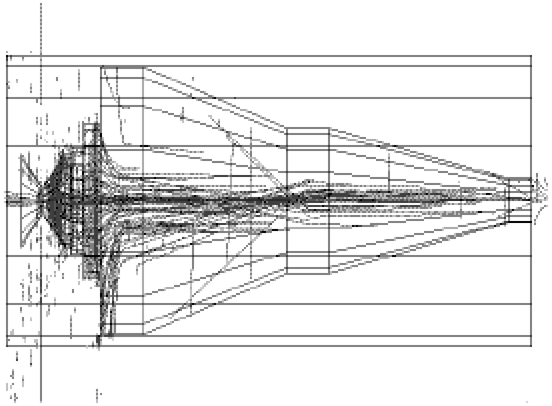

Figure 5: Positron tracks in the aperture of the $\beta^* = 3$ mm IR lattice (Fig. 4) for hundred 2-TeV μ^+ decays distributed uniformly in the 150-m IR. No sweep dipoles in the lattice. Aperture scale: 10 cm radially and 150 m longitudinally.

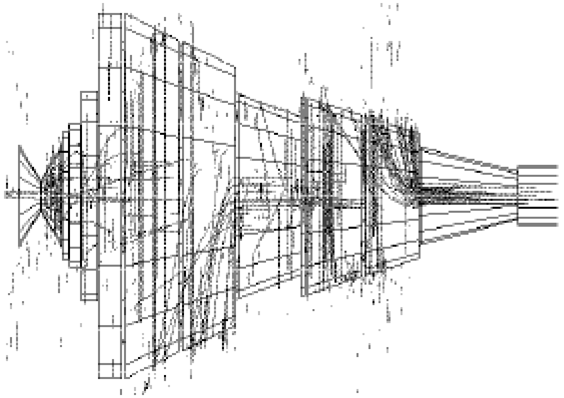

Figure 6: Positron tracks in the aperture of the $\beta^* = 3$ mm IR lattice (Fig. 4) for hundred 2-TeV μ^+ decays distributed uniformly in the 150-m IR. Four 8.5 T sweep dipoles are in the lattice. Aperture scale: 10 cm radially and 150 m longitudinally.

Results: Combined Approach continued…

- Top performing IR design and comparisons of dependence of heat dissipation in IR and shielding design approaches-

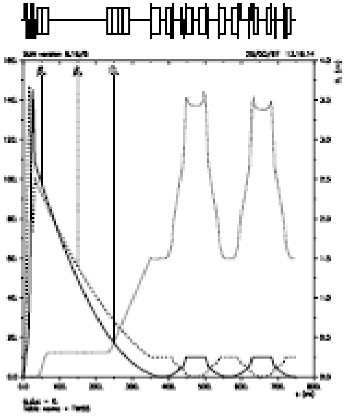

Figure 1: Horizontal (solid line) and vertical (dashed line) β-functions in the $\beta^* = 3$ mm IR lattice. Dot-dashed line shows the dispersion.

Table I: Power dissipation (W/m) in the 4σ IR components. $\beta^* = 3$ mm 270 m lattice with a 3-cm tungsten liner inside the SC magnets (May 1996).

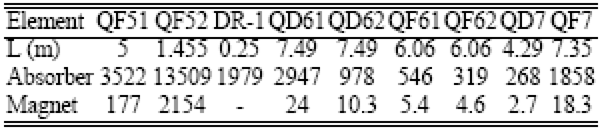

Element	QF51	QF52	DR-1	QD61	QD62	QF61	QF62	QD7	QF7
L (m)	5	1.455	0.25	7.49	7.49	6.06	6.06	4.29	7.35
Absorber	3522	13509	1979	2947	978	546	319	268	1858
Magnet	177	2154	-	24	10.3	5.4	4.6	2.7	18.3

Table II: Power dissipation (W/m) in the 4σ IR components. $\beta^* = 3$ mm 150 m lattice with a 3-cm tungsten liner inside the SC magnets (July 1996).

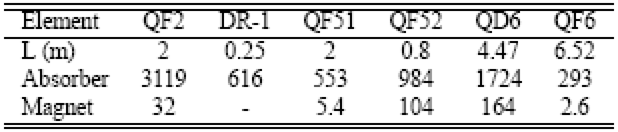

Element	QF2	DR-1	QF51	QF52	QD6	QF6
L (m)	2	0.25	2	0.8	4.47	6.52
Absorber	3119	616	553	984	1724	293
Magnet	32	-	5.4	104	164	2.6

Table III: Power dissipation (W/m) in the 5σ IR components. $\beta^* = 3$ mm 150 m lattice with a 2-cm tungsten liner inside the SC magnets, 4σ tungsten collimators, four 8.5 T sweep dipoles (August 1996).

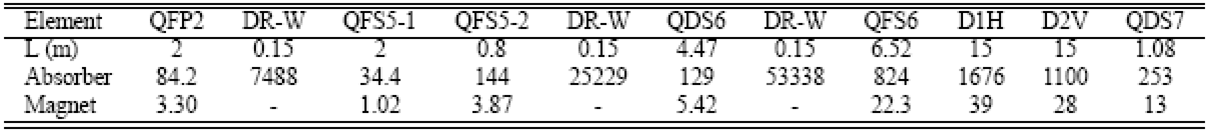

Element	QFP2	DR-W	QFS5-1	QFS5-2	DR-W	QDS6	DR-W	QFS6	D1H	D2V	QDS7
L (m)	2	0.15	2	0.8	0.15	4.47	0.15	6.52	15	15	1.08
Absorber	84.2	7488	34.4	144	25229	129	53338	824	1676	1100	253
Magnet	3.30	-	1.02	3.87	-	5.42	-	22.3	39	28	13

Detectors…

- Central detector backgrounds…

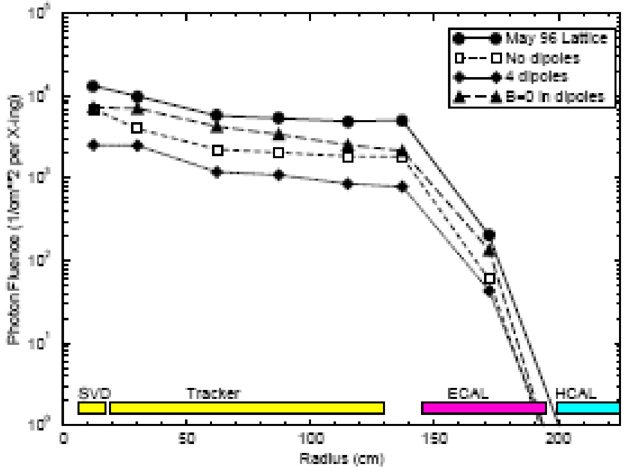

Figure 7: Radial dependence of photon fluence in the ±1.2 m central detector region around the IP per 2 × 2 TeV $\mu^+\mu^-$ bunch crossing for different IR scenarios due to muon beam decays.

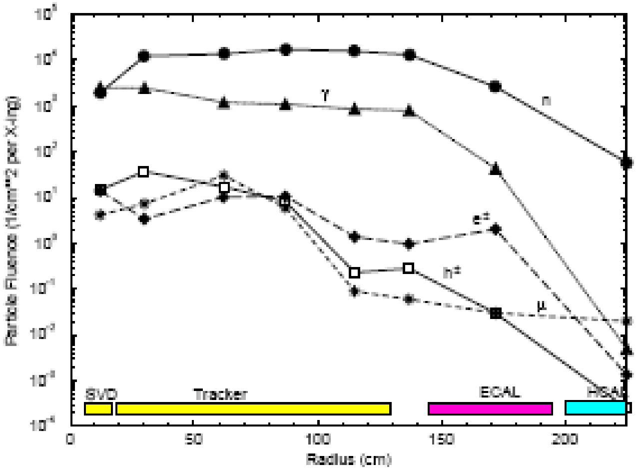

Figure 8: Radial dependence of particle fluence in the ±1.2 m central detector region around the IP per 2 × 2 TeV $\mu^+\mu^-$ bunch crossing for the best IR configuration considered.

Neutrinos

- Serious problem with Bethe-Heitler pairs: 15 to 90 m from the IP is responsible for high muon fluxes in the calorimeter
  - Approaches include magnetized shielding across the entire tunnel cross section, timing cuts
  - Neutrino fluxes outside are also a problem – every meter may require a dipole or an oscillation of the guide field in time to move the beam within the accelerator

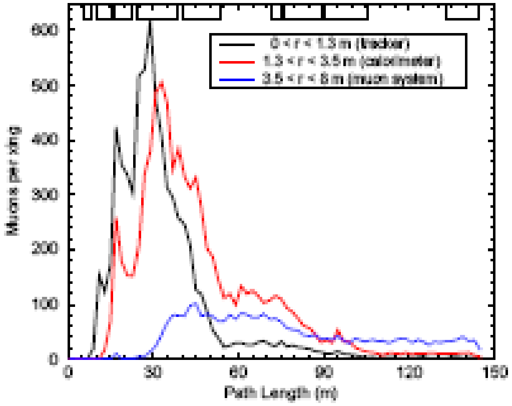

Figure 3: Number of secondary muons coming to three detector regions as a function of distance from IP of 2 TeV muon decays.

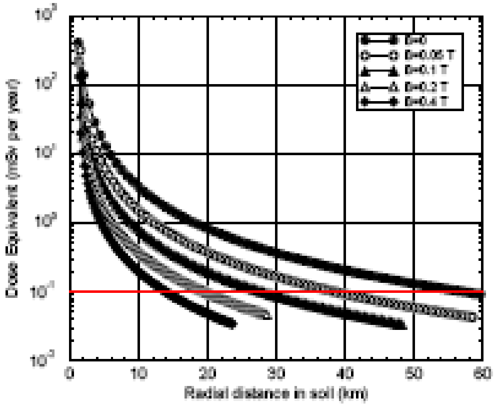

Figure 4: Neutrino induced average dose in the orbit plane vs distance in soil from the ring center for five values of the vertical wave field.

Final Comment

- We have backgrounds for 50x50 GeV, 250x250 GeV, and 2 x 2 TeV Colliders
- The most serious problem was the 250x250 GeV collider. Backgrounds were never solved
- This implies the 750x750 GeV collider under design is likely to have more severe background issues than the 2x2 TeV collider extensively studied.